



Title	Effects of guest hydrophobic molecule on stability of ordered meso structure of a surfactant/water system
Author(s)	Imai, Masayuki; Teramoto, Takashi; Takahashi, Ikuko; Nishiura, Yasumasa
Citation	Journal of Chemical Physics, 119(7), 3891-3895 https://doi.org/10.1063/1.1591734
Issue Date	2003
Doc URL	http://hdl.handle.net/2115/5430
Rights	Copyright © 2003 American Institute of Physics
Type	article
File Information	JCP119-7.pdf



[Instructions for use](#)

Effects of guest hydrophobic molecule on stability of ordered meso structure of a surfactant/water system

Masayuki Imai^{a)}

Faculty of Science, Ochanomizu University, Tokyo, 112-0012, Japan

Takashi Teramoto

Meme Media Laboratory, Hokkaido University, Sapporo 060-0813, Japan

Ikuko Takahashi

Graduate School of Humanities and Science, Ochanomizu University, Tokyo, 112-0012, Japan

Yasumasa Nishiura

Research Institute for Electronic Science, Hokkaido University, Sapporo 060-0812, Japan

(Received 11 March 2003; accepted 21 May 2003)

Addition of hydrophobic guest molecule ($C_{12}H_{26}$) into the nonionic surfactant/water system ($C_{16}E_7/D_2O$) system modifies the phase behavior between the lamellar and column phases. The distribution of the added guest molecule in the microstructure and the interfacial structure is examined by using a small angle neutron scattering technique. The characteristic length and the interfacial thickness of the microstructure are deformed in order to optimize the distribution of the guest molecules. The obtained experimental results including the existence of the double gyroid and rhombohedral phases are in agreement with those of the simple model of diblock copolymers. © 2003 American Institute of Physics. [DOI: 10.1063/1.1591734]

INTRODUCTION

Block copolymers and surfactant/water systems show various ordered meso-phases such as body centered cubic spheres (B), columns (C), lamellar (L), and double gyroid (DG) phases. These structures are stabilized by the balance of the interfacial energy and conformational entropy of molecular chains. By changing the external environment, the balance is easily modified and the system shows an order–order transition so as to minimize the free energy. Especially, the addition of guest molecules to the ordered meso-phases modifies the conformations of the molecular chains in the microstructure and brings a unique order–order transition. In this context there are extensive studies on the phase behavior of block copolymer/homopolymer (BCP/HP) blends.¹ The distribution of homopolymer within the microstructure determines the equilibrium structure and eventually produces complex new morphologies. Actually, Landh reported a parade of the cubic minimal surfaces $DG \rightarrow DD$ (double diamond) $\rightarrow DP$ (double primitive) $\rightarrow C(P)$ (Neovious) in the pine oil monoglycidides-poloxamer 407 block copolymer–water system with increasing of the water content.² Recently Dotera showed a similar cubic phase sequence in BCP/HP blend using a Monte Carlo simulation technique.³ One of the most successful theories, on the other hand, is the self-consistent mean field theory applied to BCP/HP blends.⁴ A plausible explanation of the guest molecule induced order–order transition is change of the spontaneous curvature due to the distribution of the guest molecule inside of the micro-

structure. Those calculations, however, run the risk of overlooking complex three-dimensional morphologies that has not been previously well-identified.

From these considerations, the purpose of this study is to elucidate the guest molecule induced order–order transition in the surfactant/water/hydrophobic guest molecule system from experimental and theoretical points of view. First we make clear a phase behavior of the ternary mixture system. The obtained experimental results are investigated in terms of a simple model which allows us to study it analytically. The key factor in understanding the morphology phase behavior is that the effects of the added guest molecule is interpreted as a change of the interfacial thickness. We will examine the distribution of the added guest molecule in the microstructure and the interfacial structure using a small angle neutron scattering (SANS) technique.

EXPERIMENT

In this study we added $C_{12}H_{26}$ (*n*-dodecane) into a binary mixture of D_2O and $C_{16}E_7$. It should be noted that the alkyl chain length of $C_{12}H_{26}$ is slightly shorter than that of $C_{16}E_7$. The nonionic surfactants $C_{16}E_7$ (purity >98%) and (purity >98%) dodecane were purchased from Nikko Chemicals Inc. and Kanto Chemical Co., Ltd., respectively, and used without further purification. The phase behavior of the $C_{16}E_7/D_2O$ system is well characterized by Kato *et al.*⁵ The ternary mixture samples for the SANS measurements were prepared by the following procedure. The surfactant and water mixtures were homogenized and then dodecane was added to the surfactant solution at room temperature (column phase). The ternary mixture samples were monophasic and transparent in the observed temperature region. SANS mea-

^{a)}Electronic mail: imai@phys.ocha.ac.jp

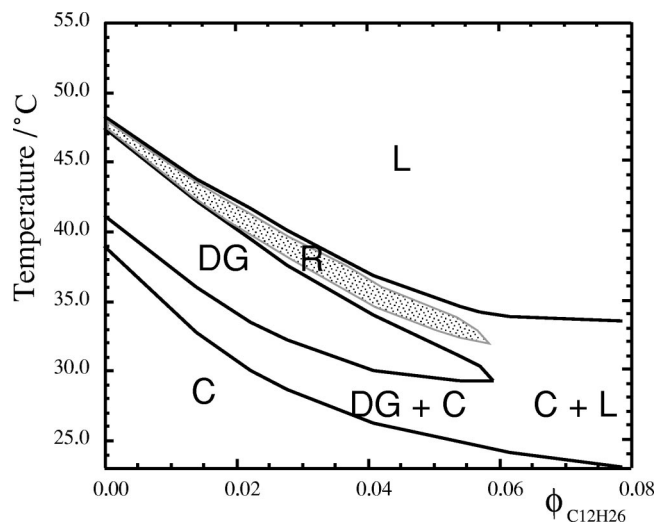


FIG. 1. Phase diagram for $C_{16}E_7/D_2O/C_{12}H_{26}$ system. The R phase of the gray region is observed during the process of the $L \rightarrow DG$ transition.

measurements were performed using a SANS-U instrument of the Institute for Solid State Physics, The University of Tokyo at JRR-3M of the Japan Atomic Energy Research Institute.⁶ In this experiment we used 7.0 Å wavelength neutron beam with the wavelength resolution $\Delta\lambda/\lambda$ of 10%. The obtained scattering profiles were corrected for the nonuniformity, background scattering, and incoherent scattering from protonated substances. A differential scanning calorimeter (DSC) apparatus Seiko DSC6100 and a small angle x-ray scattering (SAXS) apparatus Rigaku NANO-Viewer-IP with confocal mirror were used to examine the phase behavior of the ternary mixture samples. For the DSC measurements, the samples with about 60 mg weight were sealed in silver DSC pans used for liquid samples. Samples were heated from room temperature ($\sim 25^\circ\text{C}$) to 80°C at fixed heating rates $0.5^\circ\text{C}/\text{min}$. The obtained DSC diagrams were calibrated using standard sapphire sample. The SAXS measurements were performed using a point focusing camera with $\text{Cu } K\alpha$ radiation. The scattering patterns were recorded on a 1024×1024 pixels two-dimensional imaging plate covering the scattering vector q ($q = 4\pi \sin \theta/\lambda$) range from 0.03 to 0.30 \AA^{-1} .

RESULTS AND DISCUSSIONS

Addition of the hydrophobic guest molecule ($C_{12}H_{26}$) into the 55 wt % $C_{16}E_7/D_2O$ system modifies the phase behavior. Figure 1 shows the temperature- $\phi_{C_{12}H_{26}}$ ($\phi_{C_{12}H_{26}}$: volume fraction of dodecane) phase diagram of the ternary system at 55 wt % $C_{16}E_7$ solution and the corresponding SAXS profiles are shown in Fig. 2. Without the guest molecule, the system shows a typical morphology sequence $L \rightarrow \text{MFL} \rightarrow R \rightarrow DG \rightarrow C$, where MFL and R phases designate a modulation fluctuation layer structure and a rhombohedral network structure, respectively. The two morphologies are characteristic intermediate structure observed in L to DG transition of nonionic surfactant/water systems. Especially the R phase has $R\bar{3}_c$ symmetry which is subgroup of $I_{a\bar{3}d}$ symmetry for the DG phase, indicating that the R phase

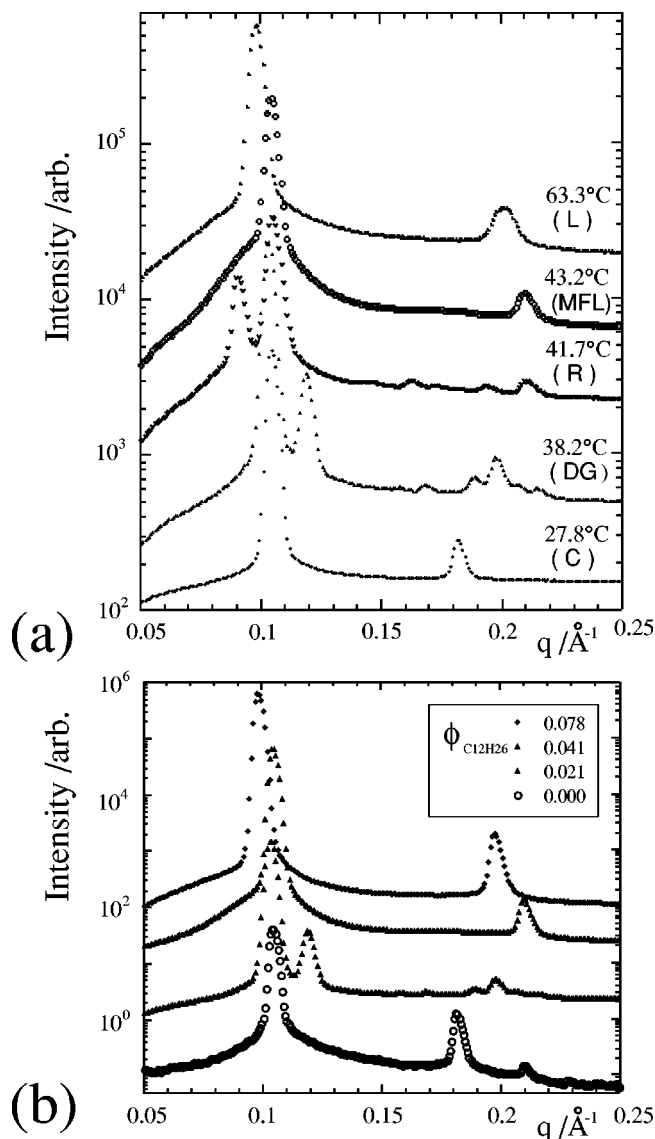


FIG. 2. (a) Dependence of scattering intensity on temperature at $\phi_{C_{12}H_{26}} = 0.03$. (b) Dependence of scattering intensity on added $C_{12}H_{26}$ volume fraction at 38.5°C .

plays an important role in the kinetic pathway from L to DG transition.⁷ Addition of the guest molecule until $\phi_{C_{12}H_{26}} \sim 0.03$ does not affect the morphology sequence as shown in Fig. 2(a). However, when $\phi_{C_{12}H_{26}}$ exceeds ~ 0.06 , R and DG phases disappear on the phase diagram and the L phase transforms to the C phase directly by changing the temperature. Thus with increasing $\phi_{C_{12}H_{26}}$, the system shows the morphology transition $C \rightarrow DG \rightarrow L$ as shown in Fig. 2(b). The L phase is stabilized by the addition of the guest molecule, whereas the DG and R phases are destabilized and finally disappear on the phase diagram. This experimental observation shows good agreement with the phase diagram of BCP/HP blends obtained by Matsen.⁴ In the case of the L phase, according to the reference, the segregation between copolymers and homopolymers enhances order of the lamellar phase and increases the lamellar spacing, resulting in the stabilization of the L phase.

One of the requirements to describe the qualitative phase

behavior observed in our surfactant/water system as well as copolymers is that it captures the most essential physics of the ordered phase under consideration while the model should be free from the details of the system thanks to the isotropy. Recall that in our system the R phase is observed between the L and DG phases. Another requirement for the successful framework is that the existence and stability of the DG and R phases can be realized by the simple model. Then we apply the following model to describe the phase behavior of the ordered meso-structures.

By minimizing the Cahn–Hilliard type equations of the free-energy functional $F_{\epsilon,\sigma}$, both the DG and R morphologies are dictated in some parameter region of the Ohta–Kawasaki model for diblock copolymers,^{8–10}

$$F_{\epsilon,\sigma}(u) = \int_{\Omega} \left(\frac{\epsilon^2}{2} |\nabla u|^2 + W(u) + \frac{\sigma}{2} |(-\Delta)^{-1/2}(u - \bar{u})|^2 \right) d\mathbf{r}, \quad (1)$$

where $\bar{u} = |\Omega|^{-1} \int_{\Omega} u d\mathbf{r}$ and $(-\Delta)^{-1/2}$ is a fractional power of the Laplace operator. The phase function u describes roughly the microscopic state of the polymers relevant to its transition between phases. The notation Ω represents the physical space which is taken to be the unit cube $[0:1]^3$, and $W(u)$ is set to the form $(u^2 - 1)^2/4$. The first term minimizes unfavorable interfaces and the third term avoids overstretching the polymer blocks. The period of the minimizer is a meso-scale between results from the competition described earlier. We set appropriately to $\sigma/\epsilon = 2^{11}(1 - \bar{u}^2)^{-2}$ in order to consider a periodic structure in space with Ω being its unit domain.¹⁰ The parameter ϵ thus represents the rescaled interfacial thickness (corresponding to the ratio of the interface thickness to the layer interval).

Figure 3(a) illustrates the phase diagram obtained numerically from the comparison of the $F_{\epsilon,\sigma}(\bar{u})$ between the candidate structures. For nonparallel layers, we compare the $F_{\epsilon,\sigma}$ values with $|\Omega|$ changing slightly in order to select the lowest-energy morphology. The L phase is stable for small ϵ , whereas the R and DG phases are stable for large ϵ . In the limit of $\epsilon \searrow 0$, the contributions from each term of $F_{\epsilon,\sigma}$ are equally balanced in the order of $O(\epsilon)$.¹⁰ The small ϵ regime of the phase diagram of Fig. 3(a) is consistent with the phase behavior of Fig. 1. The local phase behavior obtained from the skeleton model investigated here can be applied to describe roughly a variety of behaviors between the ordered meso-phases.

The morphology of the system for large ϵ , on the other hand, can be determined by the area minimization of the interface region, whereas its characteristic layer spacing and enclosed region has a fixed length and volume, respectively. They, therefore, are close to the constant mean curvature surfaces. We denote here the interface by the level set of $\Gamma \equiv \{\mathbf{r} \in \Omega : u(\mathbf{r}) = \bar{u}\}$. As shown in Table I, a border—whether the area Γ of the R morphology is smaller than that of DG—falls in the region around $\bar{u} = 0.10$ (The area Γ of L is $2^{5/2}$). This is in good agreement with the R-DG transition line of the phase diagram of Fig. 3(a).

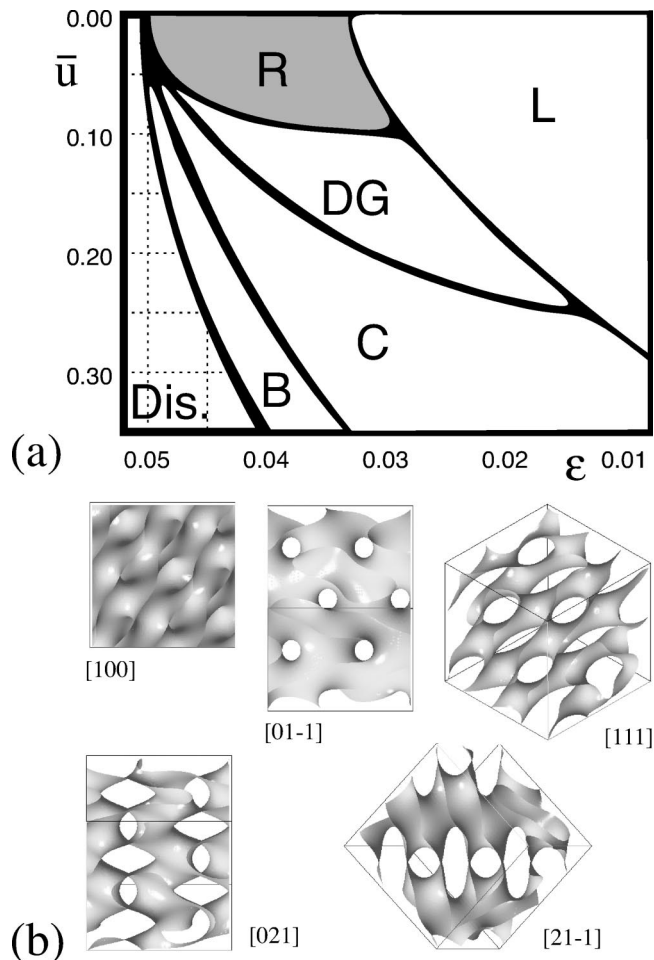


FIG. 3. (a) The \bar{u} – ϵ phase diagram of the stable morphology when $\sigma/\epsilon = 2^{11}(1 - \bar{u}^2)^{-2}$. (b) The views of the rhombohedral morphology from the various directions. All figures show the isosurfaces at $\bar{u} = 0.10$.

In this connection, it is worth noting some geometrical measures¹¹ of the R morphology. We estimate that 80% of the total surface has zero or negative Gaussian curvature K for $\epsilon = 0.04$ (67% for $\epsilon = 0.01$). The interface Γ of R, in the other words, has saddle shaped areas everywhere. The Euler characteristic $\chi (\equiv (2\pi)^{-1} \int_{\Gamma} K dS)$ is -24 , in which the unit cell investigated here is shown in Fig. 3(b). The local mean curvatures for $\epsilon = 0.04$, on the other hand, distributes around the zero value rather sharply than that for $\epsilon = 0.01$. When $\bar{u} = 0.00$, in particular, the mean curvature of the R morphology approaches into the zero value, while that of DG is 1.84. The details will be reported somewhere. We assert that the stabilization of the DG and R phase is dominated by the ratio of the interface thickness to the layer interval.

The theoretical results described above have been confirmed experimentally as follows: We examined degree of order and membrane thickness as a function of guest molecule concentration. This ternary mixture system consists of hydrogenated surfactant, hydrogenated hydrophobic guest molecule, and deuterated water. In the mixture the hydrophilic part of the bilayer is swollen by the deuterated water like the polymer swollen brush.^{12,13} Thus the system can be described by a three layer model consisting of a water layer, hydrophilic interfacial layer, and hydrophobic layer (hydro-

TABLE I. The \bar{u} dependence of area Γ and integral of mean curvature H ($\int_{\Gamma} H dS$) near the DG-R transition region.

\bar{u}	Area Γ				$\int_{\Gamma} H dS$	
	$\epsilon=0.01$		$\epsilon=0.04$		$\epsilon=0.04$	
	DG	R	DG	R	DG	R
0.00	5.570	5.336	5.353	5.293	9.878	0.197
0.05	5.497	5.308	5.306	5.270	10.097	4.821
0.08	5.450	5.287	5.275	5.257	10.298	5.795
0.09	5.435	5.279	5.261	5.253	10.178	6.075
0.10	5.420	5.272	5.250	5.248	10.238	6.326
0.11	5.405	5.264	5.239	5.242	10.301	6.558
0.12	5.389	5.256	5.228	5.237	10.367	6.774
0.15	5.339	5.230	5.192	5.219	10.570	7.534

phobic group of the surfactant and hydrophobic guest molecule). In order to extract the structural parameters, the scattering profiles for the L phase of $C_{16}E_7/D_2O/C_{12}H_{26}$ system at $57.5^\circ C$ were fitted by the model scattering function for the lamellar structure proposed by Nallet *et al.*,¹⁴

$$I_{\text{powd}} \sim \frac{N}{q^2} P(q) S(q), \quad (2)$$

$$P(q) = \frac{2(\Delta\rho)^2}{q^2} [1 - \cos(q\delta) \exp(-q^2\sigma^2/2)], \quad (3)$$

$$S(q) = 1 + 2 \sum_{n=1}^{N-1} \left(1 - \frac{n}{N}\right) \cos\left(\frac{qdn}{1 + 2(\Delta q)^2 d^2 \alpha(n)}\right) \times \exp\left[-\frac{2q_z^2 d^2 \alpha(n) + (\Delta q)^2 d^2 n^2}{2(1 + 2(\Delta q)^2 d^2 \alpha(n))}\right] \times \frac{1}{\sqrt{1 + 2(\Delta q)^2 d^2 \alpha(n)}}, \quad (4)$$

where N is the number of lamellar layers, $\Delta\rho$ is the contrast between the hydrophobic part of bilayer with width δ (including thickness of hydrophobic guest molecule layer) and the solvent and the Δq is the width of the resolution function assuming a Gaussian profile. The interface thickness σ is defined as the Gaussian distribution width for δ . The $\alpha(n)$ is a correlation function for undulating lamellae expressed by $\alpha(n) = (\eta/4\pi^2)[\ln(\pi n) + \gamma]$ with Euler's constant γ . Caillé parameter η is given by $q_0^2 k_B T / 8\pi \sqrt{K\bar{B}}$ where K is the bulk bending modulus, \bar{B} is the bulk modulus for layer compression, and q_0 is the position of first Bragg singularity, $q_0 = 2\pi/d$. Without the guest molecule, the scattering profile gave the following parameters, $d = 59.1 \text{ \AA}$, $\delta = 23.3 \text{ \AA}$, $\sigma = 3.2 \text{ \AA}$, and $\eta = 0.25$. Using the simple dilution law $d = \delta / \phi_{C_{16}E_7}$ ($\phi_{C_{16}E_7}$: volume fraction of $C_{16}E_7$), the thickness of the bilayer can be estimated as 34.6 \AA . This value agrees with the value of $\delta + 4\sigma = 36.1 \text{ \AA}$, since in this model the hydrophilic part of the surfactant exists in the interfacial region. The interlamellar interaction of the nonionic surfactant/water system is governed by the Helfrich interaction,¹⁵ which gives a simple relationship among the Caillé parameter, membrane thickness, and lamellar spacing by $\eta = 4(1 - \delta/d)^2/3$. When we use $\delta = 34.6 \text{ \AA}$, and d

$= 59.1 \text{ \AA}$, we obtain $\eta = 0.23$, which agrees well with the fitting value of 0.25. Thus the pure $C_{16}E_7/D_2O$ system is well described by the three layer model.

Figure 4(a) shows the variation of the hydrophobic layer thickness δ as a function of the volume fraction of the guest molecule $\phi_{C_{12}H_{26}}$. A solid line in Fig. 4(a) is the expected dependence of the hydrophobic layer thickness assuming that the added guest molecules are completely segregated in the

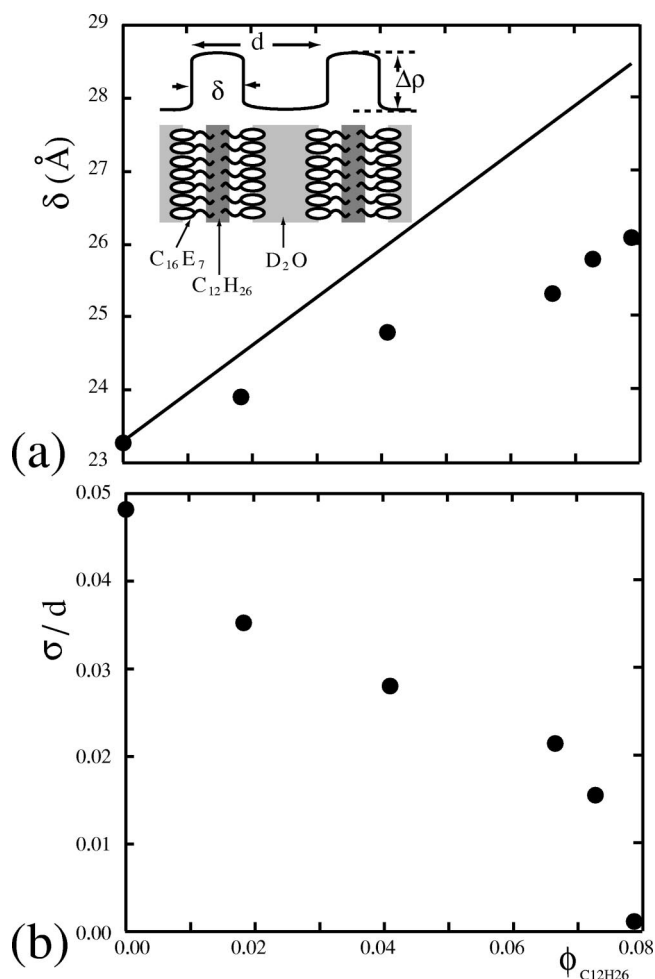


FIG. 4. (a) Dependence of hydrophobic width on added $C_{12}H_{26}$ volume fraction and schematic illustration of a three layer model. (b) Dependence of interfacial thickness on added $C_{12}H_{26}$ volume fraction.

center of the bilayer. In this calculation, we used incompressibility of each molecule and molecular volumes of the functional groups.¹² The hydrophobic layer width δ increases linearly as $\phi_{C_{12}H_{26}}$ increases, although the values are somewhat smaller than the expected values assuming complete segregation. Thus the $C_{12}H_{26}$ molecule is mostly segregated from the hydrophobic part of surfactant molecules, but partially penetrates into the hydrophobic part. This segregation might bring the sharp distribution of the hydrophobic group in the bilayer and enhance the order of bilayer, since the Caillé parameter η decreases with increasing $\phi_{C_{12}H_{26}}$. On the other hand, the partially penetrated molecule increases the surface area per surfactant molecule, which decreases the thickness of the hydrophilic part due to the connectivity. The ratio σ/d of the interfacial thickness to the lamellar spacing decreases with the addition of hydrophobic guest molecules as shown in Fig. 4(b). Thus the addition of the hydrophobic guest molecules into the surfactant/water system brings a sharp boundary of the surfactant bilayer, which causes the order–order transition as predicted by the numerical calculation phase diagram of Fig. 3(a).

In summary, we studied the morphology phase behavior of the $C_{16}E_7/D_2O/C_{12}H_{26}$ ternary mixture system and discussed qualitatively the effect of the added guest molecule to the interface structures based on the skeleton model for

diblock copolymers. In order to optimize the distribution of the guest molecules, the spacing between layers increases and the rescaled interfacial thickness decreases with increasing the addition of the guest molecules, resulting in the disappearance of the DG and R phases for small ϵ . The agreement between our experiments and numerical results lends further support to our assertion that the rescaled interface thickness is regarded as a factor to determine the ordered meso-phase of the system.

¹For examples, I. W. Hamley, *The Physics of Block Copolymers* (Oxford University Press, New York, 1998).

²T. Landh, *J. Phys. Chem.* **98**, 8453 (1994).

³T. Dotera, *Phys. Rev. Lett.* **89**, 205502 (2002).

⁴M. W. Matsen, *Macromolecules* **28**, 5765 (1995).

⁵T. Kato *et al.*, *Langmuir* **11**, 4661 (1995).

⁶Y. Ito, M. Imai, and S. Takahashi, *Physica B* **213–214**, 889 (1995).

⁷M. Imai *et al.*, *J. Chem. Phys.* **115**, 10525 (2001).

⁸T. Ohta and K. Kawasaki, *Macromolecules* **19**, 2621 (1986).

⁹Y. Nishiura and I. Ohnishi, *Physica D* **84**, 31 (1995).

¹⁰T. Teramoto and Y. Nishiura, *J. Phys. Soc. Jpn.* **72**, 1611 (2002).

¹¹M. Fiałkowski, A. Aksimentiev, and R. Holyst, *Phys. Rev. Lett.* **86**, 240 (2001).

¹²K. Minewaki *et al.*, *Langmuir* **17**, 1864 (2001).

¹³S. T. Milner, T. A. Witten, and M. E. Cates, *Macromolecules* **21**, 2610 (1988).

¹⁴F. Nallet, R. Laversanne, and D. Roux, *J. Phys. II* **3**, 487 (1993).

¹⁵W. Helfrich, *Z. Naturforsch. A* **33a**, 305 (1978).